Annexin A2 recognises a specific region in the 3′-UTR of its cognate messenger RNA

Hanne Hollås, Ingvild Aukrust, Stine Grimmer [1], Elin Strand, Torgeir Flatmark, Anni Vedeler *

Department of Biomedicine, University of Bergen, Jonas Lies vei 91, N-5009 Bergen, Norway

Abstract

Annexin A2 is a multifunctional Ca^{2+}- and lipid-binding protein. We previously showed that a distinct pool of cellular Annexin A2 associates with mRNP complexes or polysomes associated with the cytoskeleton. Here we report in vitro and in vivo experiments showing that Annexin A2 present in this subset of mRNP complexes interacts with its cognate mRNA and c-*myc* mRNA, but not with β_2-*microglobulin* mRNA translated on membrane-bound polysomes. The protein recognises sequence elements within the untranslated regions, but not within the coding region, of its cognate mRNA. Alignment of the Annexin A2-binding 3′-untranslated regions of *annexin* A2 mRNA from several species reveals a five nucleotide consensus sequence 5′-AA(C/G)(A/U)G. The Annexin A2-interacting region of the 3′-untranslated region can be mapped to a sequence of about 100 nucleotides containing two repeats of the consensus sequence. The binding elements appear to involve both single and double stranded regions, indicating that a specific higher order mRNA structure is required for binding to Annexin A2. We suggest that this type of interaction is representative for a group of mRNAs translated on cytoskeleton-bound polysomes.
© 2006 Elsevier B.V. All rights reserved.

Keywords: Annexin A2; mRNA; 3′-UTR; mRNA-binding; consensus sequence; c-*myc*

1. Introduction

In eukaryotic cells mRNA-binding proteins modulate gene expression by regulating the activity, abundance and stability of both the coding and non-coding mRNAs present in mRNP complexes. These proteins contribute to the organisation of mRNAs into structurally and functionally related subsets of such complexes, thus coordinating mRNA localisation and the synthesis of proteins involved in complex cellular processes

[1–4]. Most of the localised mRNAs require components of the cytoskeleton for their transport from the nucleus to specific target sites in the cell. Both actin filaments and microtubules, and their associated motor molecules, play a role in mRNA targeting. In general, the targeting signal resides in the 3′-UTRs of the mRNAs. In the case of *Vg1* and *actin* mRNAs, these elements (also referred to as Zip codes) are small single stranded RNA (ssRNA) sequences [5,6]. However, the precise targeting sequences are often difficult to define since they are most likely related to a higher order structure of the mRNAs. Accordingly, secondary structures within *cis*-acting elements, in association with *trans*-acting proteins, have been implicated in the targeting of most mRNAs [7]. Different steps in the localisation of mRNAs are often mediated by separate *cis*-acting elements. For example, a sequence of 11 nucleotides (nt) is sufficient to direct the transport of *myelin basic protein* mRNA from the cell body into the oligodendrocyte processes, whereas another region of approximately 340 nt, containing a stable secondary structure, mediates its localisation to the myelin compartment [8]. Repression of translation during the transport process ensures that protein expression occurs selectively at the target site [1]. For

example, it has been shown that only localised *nos* mRNA, which codes for the Nanos protein in *Drosophila*, is translated [9].

A 3′-UTR-binding protein, in complex with other proteins, is involved in the targeting of β-*actin* mRNA to actin filaments in fibroblasts [3,10]. A homologue of this protein targets *Vg1* mRNA to microtubules in *Xenopus* oocytes [11]. Hence, alternative filament-associated proteins appear to determine the specificity of the association of distinct mRNAs with the cytoskeleton. Annexin A2 (AnxA2) may function as such a protein since it has been identified both as a F-actin-binding [12–14] and a mRNA-binding protein [15–17], associated with a specific subpopulation of mRNP complexes [15]. Interestingly, regulation of mRNA-cytoskeleton interactions would only be one of the cellular roles of this multifunctional protein, which has also been implicated in signal transduction, membrane trafficking and regulation of membrane/cytoskeleton contacts [18–22].

We have previously developed a method for the isolation of three specific subpopulations of polysomes from cultured cells, i.e. "free" (or loosely cytoskeleton-bound; FP), cytoskeleton-bound (CBP) and membrane-bound polysomes (MBP) [23]. This well-characterised fractionation protocol [15,24–29] made it possible to analyse the compartmentalisation of specific mRNAs and study their interactions with the cytoskeleton. As a result of such analysis, AnxA2 was identified as a mRNA-binding protein in the CBP fractions [15]. Since c-*myc* mRNA is translated on CBP in Krebs II cells [24] and fibroblasts [25], the identity of the components mediating the interaction of c-*myc* and other specific mRNAs with the CBP was further studied. Here we show that AnxA2 in mRNP complexes is associated with c-*myc* and *anx*A2 mRNAs translated on CBPs in vivo. Moreover, we provide evidence supporting the conclusion that AnxA2 interacts with a ~100 nt region in the 3′-UTR of its cognate mRNA.

2. Materials and methods

2.1. Cell fractionation and isolation of polysomes

Three subpopulations of polysomes were isolated from Krebs II cells essentially as described [23].

2.2. Northern blot analysis

Total RNA was isolated from each of the three individual polysomal subpopulations purified from Krebs II cells by the single-step guanidinium–isothiocyanate–phenol–chloroform extraction method [30]. The conditions for Northern blotting were essentially as described by Hesketh et al. [25]. The probes were generated from bovine *anx*A2 (corresponding to a sequence in the N-terminal coding region with 86% homology to the same region in mouse *anx*A2), mouse c-*myc* or β₂-*microglobulin* cDNAs using Multiprime kits and R[α-³²P]dCTP (3000 Ci/mmol), both obtained from Amersham Pharmacia Biotech.

2.3. Immunoprecipitation and reverse trancriptase polymerase chain reaction (RT-PCR)

Immunoprecipitation of AnxA2–mRNP complexes was performed essentially as published by Chu et al. [31]. In brief, Krebs II cells were fractionated as described [23] and 1.5 mg of the cytoskeletal fraction was immunoprecipitated using monoclonal AnxA2 antibodies (kindly provided by Prof. Volker Gerke, Münster) coupled to protein A-Sepharose via rabbit anti-mouse IgG (RAM) after pre-clearance by RAM. The immunoprecipitation was performed in NET-buffer

(50 mM Tris–HCl, pH 7.4, 150 mM KCl and 0.05% Triton) containing 40 U/ml of RNasin (Promega). The immunoprecipitates were phenol/chloroform extracted twice. The first water-phase was incubated with RNase-free DNase (Promega) before the second extraction. Nucleic acids were precipitated with carrier tRNA and resuspended in RNase-free water. The interphase from the first phenol/chloroform extraction was resuspended in NET-buffer and acetone precipitated. AnxA2 was identified by Western blot analysis using monoclonal AnxA2 antibodies (Transduction Laboratories). Next, immunoprecipitated RNA was used as template for RT-PCR in the Access RT-PCR System (Promega) using the conditions recommended by the manufacturer. 5 μM of primers (Eurogentec) were used for the amplification of the 3′-UTRs of mouse c-*myc*, *anx*A2 and β₂-*microglobulin* cDNAs (Table 2A).

2.4. Purification of the AnxA2 heterotetramer (AnxA2t)

The AnxA2t was purified from epithelial cells derived from pig intestines as described [12].

2.5. Construction of recombinant AnxA2

The bovine *anx*A2 cDNA, originally from the pcD vector (ac. no. M14056, ATCC) [32], was cloned into the pGEM-3Zf(+) vector and used as a template for the construction of recombinant AnxA2 by PCR. The PCR product was synthesised using specific forward (5′-ATCCGGGAAGACTTCATGGG-TATGTCTACCGTTCATGAAATTCTGTGC-3′) and reverse (5′-ATCCGG-GAAGACTGGTACCTCAGTCATCCCCACCACACAGG-3′) primers obtained from Eurogentec and TIB MOLBIOL. The PCR fragment was ligated into the TOPO vector (Invitrogen) using TA cloning for amplification before digestion by restriction enzymes (*Nco*I and *Acc65I*) and ligation of the PCR product into the pETM-41 expression vector (kindly provided by Gunter Stier, EMBL, Heidelberg). The vector is derived from the pET24d expression vector (Novagen) and contains a 6His-Maltose Binding Protein tag followed by a Tobacco Etch Virus (TEV)-protease sensitive linker (ENLYFQG). DNA sequencing verified the identity of the final construct.

2.6. Protein expression and purification

The AnxA2 fusion protein (see above) was expressed overnight at 15 °C in the BL-21 *Escherichia coli* strain. Cells were harvested by centrifugation and resuspended in breakage buffer (50 mM Na₂HPO₄ (pH 8.0), 0.5 M NaCl, 10 mM imidazole, 5% (w/v) glycerol, 0.5 μg/ml DNase I, 0.25 μg/ml RNase A, protease inhibitor cocktail (1 tablet/50 ml) (Complete, EDTA-free, Roche) and 1 mM DTT). Cells were disrupted by French press (type FA-073, SLM Instruments). The homogenate was centrifuged at 100 000 g_{av} for 1 h at 4 °C, and the supernatant was loaded on His-Select Nickel Affinity Gel (Sigma) equilibrated with buffer A (50 mM Na₂HPO₄ (pH 8.0), 0.3 M NaCl and 10 mM imidazole) and incubated for 1 h at 4 °C on a rotating wheel. The resin was washed for 5 min with buffer A containing protease inhibitor cocktail (1 tablet/100 ml), then 5 min with buffer B (50 mM Na₂HPO₄ (pH 8.0), 1 M NaCl, 10 mM imidazole and protease inhibitor cocktail (1 tablet/500 ml)) and finally with buffer A containing protease inhibitor cocktail (1 tablet/500 ml) until the A_{280} had reached approximately zero. The His-tagged protein was eluted from the resin with buffer A containing 250 mM imidazole and protease inhibitor cocktail (1 tablet/500 ml). 2 mM EGTA was added to remove any traces of Ni²⁺ bound to the protein, and subsequently the eluted protein was immediately loaded on a PD-10 column (Sephadex G-25, Pharmacia) equilibrated with 20 mM Tris, pH 8. The protein was digested with TEV protease at 4 °C (molar ratio 1:50) during centrifugation at 480×*g* (overnight). Digested AnxA2 was separated from the undigested form and from His-tagged Maltose Binding Protein by loading it to Q-Sepharose (Amersham Biosciences) that had been equilibrated overnight using 100 mM Tris (pH 8) and 500 mM NaCl. The resin was washed twice in 100 mM Tris (pH 8) to remove the salt, before loading the digestion mixture to the Q-Sepharose. Due to the difference in charge between Maltose Binding Protein and AnxA2, the former binds to the Q-Sepharose while AnxA2 remains unbound. The purity of recombinant AnxA2 was determined by SDS-PAGE [33] followed by Coomassie Brilliant Blue staining and the concentration was measured spectrophotometrically by using the theoretical extinction coefficient at A_{280} of 30250 M⁻¹cm⁻¹ as determined from the amino

Table 1
DNA templates used for the in vitro generation of different *anx*A2 transcripts

*anx*A2 transcript	Restriction sites for cloning	Linearised by	Promoter
1–1381nt *anx*A2 (1)	*Bam*HI	*Eco*RI	SP6
Δ1–964nt *anx*A2 (2)	*Bam*HI–*Bgl*II	*Bgl*II	SP6
Δ55–1074nt *anx*A2 (3)	*Bam*HI–*Hind*III	*Hind*III	T7
Δ473–1381nt *anx*A2 (4)	*Pst*I–*Eco*RI	*Eco*RI	SP6
Δ473–964nt *anx*A2 (5)	*Pst*I–*Bgl*II	*Bgl*II	SP6
Δ1075–1381nt *anx*A2 (6)	*Pst*I–*Eco*RI	*Eco*RI	SP6

The respective *anx*A2 transcripts, the restriction enzyme sites used for cloning and linearisation of the templates, and the RNA polymerases used for in vitro transcription, are indicated. The numbers of the *anx*A2 transcripts in parenthesis refer to the numbers of the transcripts shown in Fig. 3. The length and the specific regions of the different *anx*A2 transcripts are shown in Fig. 3.

acid composition using the ProtParam tool (ExPASy server). Aliquots of the purified protein were stored in liquid N_2.

2.7. Preparation of cDNA templates for in vitro transcription

The bovine *anx*A2 cDNA [32], cloned into the pGEM-3Zf(+) vector, was used as a template for the construction of all the *anx*A2 transcripts. Transcripts

Fig. 1. The *anx*A2 mRNA associates with cytoskeleton-bound polysomes. The distribution of *anx*A2, c-*myc* and β_2-*microglobulin* mRNAs in RNA fractions isolated from the "free" (loosely cytoskeleton-bound; FP), cytoskeleton-bound (CBP) and membrane-bound (MBP) polysomes of Krebs II cells was determined by Northern blotting. The resulting autoradiograms are shown. 20 μg of total RNA from each fraction was loaded on the gel.

2, 4 and 5 were excised directly from the *anx*A2 cDNA using the restriction sites indicated in Table 1, while transcripts 3 and 6 were synthesised by PCR with primers (Eurogentec) containing specific restriction sites (Tables 1 and 2B). cDNAs of transcripts 1–6 were subcloned into the appropriate sites of the pGEM3Zf+ vector. All constructs were sequenced in both directions to verify the orientation and sequences of the inserts. Transcripts 7–13 were all

Table 2
Sequences of primers used in RT-PCR of AnxA2-immunprecipitated RNA in Fig. 2(A) and PCR of different *anx*A2 transcripts in Fig. 3(B)

A

Amplified fragment	Primer sequence
Δ1095–1373nt *anx*A2	5′-GTCAGAATTCAGGGCTCAGCACA-3′ (forw) 5′-CTCAGGATCCAAAGTAAAAACGGTTT-3′ (rev)
Δ1900–2265nt c-*myc*	5′-TACTGCAGACTGACCTAACTCGAGGAGG-3′ (forw) 5′-GCGGAATTCTATGGTACATGTCTTAAAATC-3′ (rev)
Δ414–862nt β2-*microglobulin*	5′-CGTCGAATTCATCAAGCATCAT-3′ (forw) 5′-CGTGAAGCTTGGTTTTTTATTTTTAG-3′ (rev)

B

*anx*A2 transcript	Primer sequence
Δ55–1074nt *anx*A2 (3)	5′-ATGTCTACCGTTCATGAAATTCT-3′ (forw) 5′-GTCAAAGCTTTCAGTCATCCCCACCA-3′ (rev)

3′UTR *anx*A2 transcripts	Primer sequence
Δ1075–1381nt *anx*A2 (6)	5′-TACTGCAGAGCCCCGCGACAGCCCAAGCA-3′ (forw) 5′-CGCGAATTCCCAACAGTAAAAATTCAG-3′ (rev)
Δ1075–1224nt *anx*A2 (7)	5′-<u>TAATACGACTCACTATAGG</u>AGCCCCGCGACAGCCCAAGC-3′ (forw) 5′-TAAACTAACAAAAGAGCGGG-3′ (rev)
Δ1225–1381nt *anx*A2 (8)	5′-<u>TAATACGACTCACTATAGG</u>GTTTCCTACGCATTACCTGG-3′ (forw) 5′-CCAACAGTAAAAATTCAGTT-3′ (rev)
Δ1075–1123nt *anx*A2 (9)	5′-<u>TAATACGACTCACTATAGG</u>AGCCCCGCGACAGCCCAAGC-3′ (forw) 5′-AGCTGGAGCACGGAGCAG-3′ (rev)
Δ1124–1224nt *anx*A2 (10)	5′-<u>TAATACGACTCACTATAGG</u>AACAGTTCTCCGCAGTCAGC-3′ (forw) 5′-TAAACTAACAAAAGAGCGGG-3′ (rev)
Δ1075–1149nt *anx*A2 (11)	5′-<u>TAATACGACTCACTATAGG</u>AGCCCCGCGACAGCCCAAGC-3′ (forw) 5′-CCGCGGGCTGACTGC-3′ (rev)
Δ1122–1143nt *anx*A2 (12)	5′-<u>TAATACGACTCACTATAGG</u>CTAACAGTTC-3′ (forw) 5′-GCTGACTGCGGA-3′ (rev)
Δ1150–1224nt *anx*A2 (13)	5′-<u>TAATACGACTCACTATAGG</u>CTAACAGCCCCCTGT-3′ (forw) 5′-TAAACTAACAAAAGAGCGGG-3′ (rev)

The length and specific regions of the different *anx*A2 transcripts are shown in Fig. 3. The T7 promoter site is underlined.
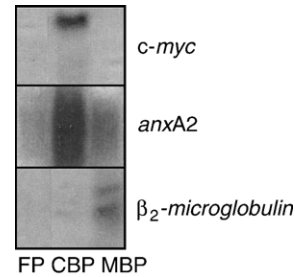
synthesised by PCR, using proof-reading RNA polymerase with forward primers (Genosys) containing the T7 promoter site (underlined in Table 2B). These transcripts were used directly for in vitro transcription.

2.8. In vitro transcription

RNA probes were uniformly [α-^{32}P]UTP-labelled (3000 Ci/mmol; Amersham Pharmacia Biotech) in vitro by transcription of linearised templates (Table 1) or PCR products (Table 2) for 90 min, by standard procedures as described in the Promega protocol. A specific activity of $1.0–2.5 \times 10^8$ cpm/μg RNA was obtained. Labelled RNA probes were analysed for integrity and purity by agarose gel electrophoresis.

2.9. AnxA2–RNA binding assays

AnxA2–RNA binding assays were performed essentially as described by Kwon and Hecht [34]. RNA was incubated with AnxA2t or recombinant AnxA2 in RNA binding solution (10 mM triethanolamine, pH 7.4, 50 mM KCl, 1 mM DTT, 2 mM MgSO$_4$, 1 mM CaCl$_2$ and 1 μg/μl of yeast tRNA), supplemented with 20 U/ml RNasin (Promega) containing 2.5% (w/v) Ficoll for 20 min in a final volume of 20 μl. After incubation, the RNA probes were covalently crosslinked to the proteins by a 10 min exposure to UV light at 5 cm distance using a Hoefer UVC 500. RNases T$_1$ and A were then added for 30 min at 37 °C to a final concentration of 0.01 U/μl and 0.1 μg/μl, respectively, to digest unprotected RNA. Nucleotide–protein complexes were separated from degraded RNA probe by 10% (w/v) SDS-PAGE [33] and visualised using a Canberra Packard Instant Imager. Coomassie Brilliant Blue staining was carried out to verify the amount of protein loaded in each lane. The binding assays of the competition experiments consisted of both radiolabelled and unlabelled competitor RNA.

3. Results

3.1. AnxA2 and c-myc mRNAs associate with CBP and AnxA2 in vivo

To identify the subpopulation of polysomes involved in translation of *anx*A2 mRNA, polysomal sub-fractionations were prepared from Krebs II cells [23,24] and Northern blot analysis was performed. The results showed that *anx*A2 mRNA is highly enriched in the CBP (Fig. 1). β$_2$-*microglobulin* mRNA, translated on MBP, and c-*myc* mRNA, translated on CBP of these cells, were used as negative and positive controls, respectively [23–25]. Further, to verify that AnxA2 interacts with c-*myc* and *anx*A2 mRNAs in intact cells, AnxA2 was immunoprecipitated from the cytoskeletal fraction of Krebs II cells, and RT-PCR of the associated RNA was performed using specific primers for the 3′-UTR regions of these mRNAs. Whereas no amplification of β$_2$-*microglobulin* cDNA was observed (Fig. 2A, lanes 14–17), this cDNA was efficiently amplified when total cellular RNA was used (Fig. 2A, lane 20), indicating that the primers and RT-PCR conditions were specific. By contrast, cDNA fragments corresponding to the 3′-UTRs of *anx*A2 and c-*myc* mRNAs were amplified (Fig. 2A, lanes 6 and 12, respectively) and their identities were confirmed by sequencing (data not shown). The specificity of immunoprecipitation
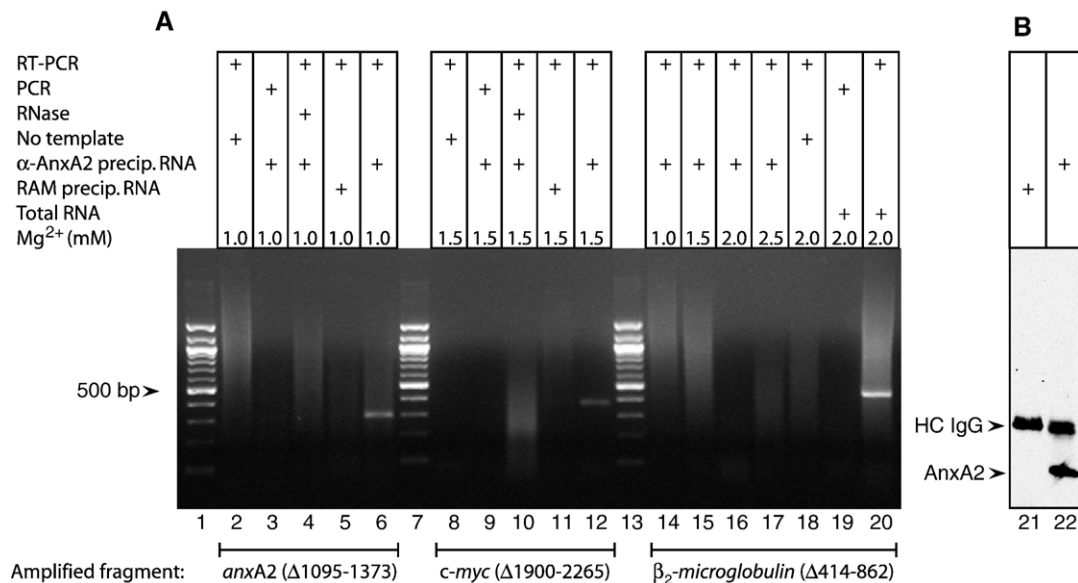

Fig. 2. *AnxA2* and c-*myc* mRNAs, but not β$_2$-*microglobulin* mRNA, associate with cytoskeleton-bound mRNPs in Krebs II cells. (A) Amplified RT-PCR/PCR products resolved on 1.8% (w/v) agarose gel stained with ethidium bromide. The AnxA2-bound mRNP complexes in the cytoskeleton fraction were immunoprecipitated using monoclonal AnxA2 antibodies (α-AnxA2) coupled to Protein A-Sepharose via RAM (lanes 3, 4, 6, 9, 10, 12, 14–17). The *anx*A2, c-*myc* and β$_2$-*microglobulin* fragments in the isolated immunoprecipitates were then RT-PCR amplified (lanes 4, 6, 10, 12, 14–17) or, as a negative control, PCR amplified (lanes 3, 9 and 19) using *anx*A2-, c-*myc*- and β$_2$-*microglobulin*-specific primers, respectively. As negative controls, the cytoskeleton fraction was also subjected to immunoprecipitation with RAM-coated Protein A-Sepharose alone and RT-PCRs were performed using the specific primers as indicated (lanes 5 and 11). As further negative controls, the immunoprecipitated samples were either treated with RNase prior to RT-PCR (lanes 4 and 10) or the RT-PCRs were performed with no template present (lanes 2, 8 and 18). No β$_2$-*microglobulin* fragment appeared after Mg^{2+} titration of the RT-PCR reaction (lanes 14–17). Therefore, the specificity of the β$_2$-*microglobulin* primers and the RT-PCR reaction conditions in the presence of 2 mM Mg^{2+} were verified using total RNA purified from Krebs II cells (lane 20). The 500 bp DNA size marker (lanes 1, 7 and 13) is indicated to the left. (B) Western blot analysis of the immunoprecipitates obtained from the cytoskeleton fraction in the absence (lane 21) or presence (lane 22) of AnxA2 monoclonal antibodies. AnxA2 was detected using monoclonal primary AnxA2 antibodies followed by HRP-coupled goat anti-mouse IgG. This secondary antibody also reacts with the heavy chain (HC) of mouse IgG present in the immunoprecipitates.

was confirmed by various RT-PCR controls (Fig. 2A) and by Western blot analysis (Fig. 2B). The latter showed that AnxA2 is present in the specific immunoprecipitates (lane 22), but not in control precipitates containing rabbit anti-mouse IgG (RAM) alone (lane 21). Similar results were obtained using total lysates of Krebs II cells (data not shown), but as expected, less mRNA was recovered in these immunoprecipitates, since only a fraction of the total cellular AnxA2 is associated with mRNPs.

3.2. Sequence elements of anxA2 mRNA involved in its binding to AnxA2

The above experiments established that AnxA2 interacts with anxA2 mRNA in vivo. Moreover, we have recently shown that it interacts directly with the localisation signal in the 3′-UTR of c-myc mRNA [17]. To establish a direct mRNA-binding and identify the region of anxA2 mRNA involved in AnxA2 binding, an UV cross-linking assay was used to monitor the
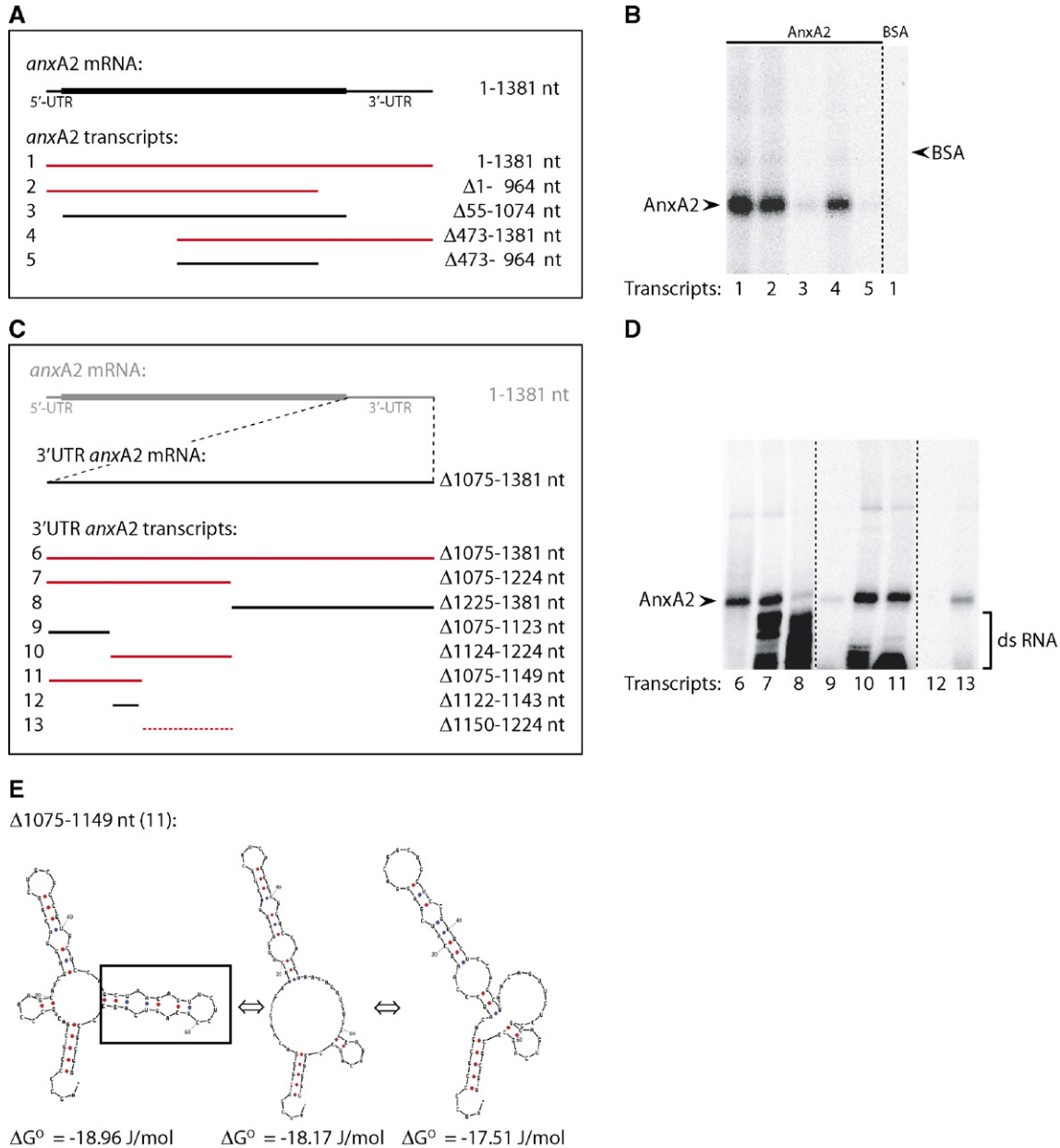

Fig. 3. Mapping of the sequence elements of anxA2 mRNA involved in its binding to AnxA2. (A) Schematic presentation of the different anxA2 transcripts generated in vitro from the full-length mRNA. The numbers to the left refer to the transcripts used in the AnxA2–RNA binding assays shown in panel B. The AnxA2-binding transcripts are shown in red. (B) The binding of 2 fmol (~100000 cpm) of the radiolabelled transcripts indicated in (A) to 2 μg of AnxA2t or BSA (lane to the right). (C) Schematic presentation of the different anxA2 3′-UTR transcripts generated in vitro. The numbers to the left refer to the transcripts used in the AnxA2–RNA binding assays shown in panel D. The AnxA2-binding transcripts are shown in red. (D) The binding of 150 fmol (~100000 cpm) of the radiolabelled transcripts indicated in (C) to 2 μg of purified recombinant AnxA2. (E) Prediction of metastable secondary structures (Mfold programme) of the Δ1075–1149 nt transcript revealed a putative stem–loop structure containing the AACAG sequence (boxed region). The AnxA2–RNA binding reactions were performed as described in Materials and methods.

binding of different in vitro radiolabelled *anx*A2 transcripts (Fig. 3A and C). As shown in Fig. 3B, full-length mRNA (transcript 1), as well as the Δ1–964 nt (transcript 2) and the Δ473–1381 nt (transcript 4) transcripts, overlapping in the coding region, were all found to bind to AnxA2t purified from porcine intestinal epithelial cells. By contrast, transcript 3, corresponding to the coding region of the *anx*A2 mRNA (Δ55– 1074 nt) (Fig. 3B) and the Δ473–964 nt transcript (Fig. 3B, transcript 5), corresponding to the coding region of transcript 4, do not interact with AnxA2. Thus, comparison of the binding activities of the different *anx*A2 transcripts indicated that a binding motif resides in the 3′-UTR (Fig. 3B, compare transcripts 3 and 5 with transcript 4). This conclusion was further supported by the binding of transcript 6 (Δ1075– 1381 nt) to AnxA2 (Fig. 3D).

Comparison of the coding region transcript 3 (Δ55–1074 nt) with the partly overlapping Δ1–964 nt transcript (Fig. 3B, compare transcripts 2 and 3), suggested that an additional binding region may reside in the 55 nt 5′-UTR of *anx*A2 mRNA. However, we were unable to confirm this by binding of the radiolabelled *anx*A2 Δ1–55 nt transcript to its cognate protein, presumably because of loss of a particular secondary

structure present in the longer RNA transcripts (data not shown). No *anx*A2 mRNA binding was observed when BSA was used in the UV cross-linking assays (Fig. 3B, lane to the right).

Since our previous results showed that AnxA2 interacts with the 3′-UTR of c-*myc* mRNA [17] and the present study shows that it also interacts with that of its cognate mRNA (Fig. 3B), it was of interest to map the binding region in the 3′-UTR of *anx*A2 mRNA in more detail. Different transcripts of the 3′- UTR of the *anx*A2 mRNA were generated by PCR using specific primers and subsequent in vitro transcription of the PCR fragments (Fig. 3C). The Δ1075–1381 nt (the entire 3′- UTR) and the Δ1075–1224 nt transcripts, but not the Δ1225– 1381 nt transcript, were found to bind to AnxA2, indicating the presence of a binding site in the 5′ end of the *anx*A2 3′-UTR (Fig. 3D, compare transcripts 6, 7 and 8). The difference between the non-binding Δ1075–1123 nt (Fig. 3D, transcript 9) and the AnxA2-binding Δ1075–1149 nt 3′-UTR region (Fig. 3D, transcript 11) is a short sequence of 26 nt, which may form a stem–loop structure (Fig. 3E, boxed region), as determined using the algorithms of the Mfold programme [35,36]. Therefore, this short nucleotide sequence could be involved in
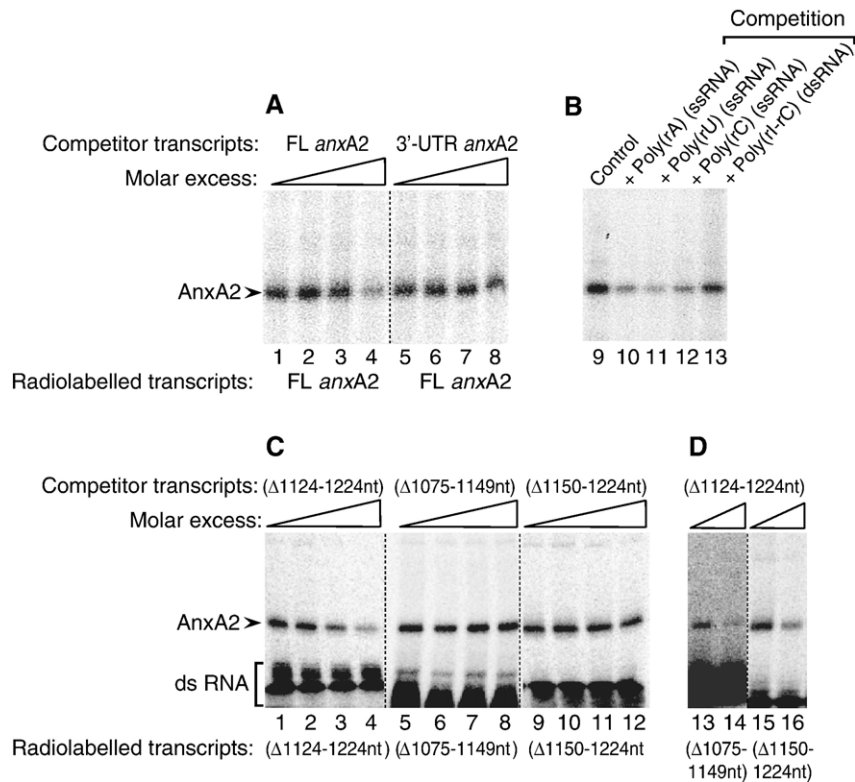

Fig. 4. Competition experiments provide evidence that AnxA2 binds to two separate regions of the *anx*A2 mRNA (A), to both ssRNA and dsRNA (B) and interacts with the Δ1124–1224 nt region of the *anx*A2 3′-UTR (C). (A) Increasing amounts (10-, 50- or 100-fold molar excess) of unlabelled in vitro transcribed full-length *anx*A2 mRNA (lanes 1–4) or *anx*A2 3′UTR (lanes 5–8) as indicated above the figure were added to 2 μg AnxA2t to compete with 1 fmol of uniformly radiolabelled full-length *anx*A2 transcript as indicated below the figure. (B) 2 μg of AnxA2t was incubated with 2 fmol of radiolabelled in vitro transcribed *anx*A2 mRNA in the absence (control, lane 9) or presence of 1 μg of either poly(rA), poly(rU), poly(rC) or poly(rI-rC) (lanes 10–13). Note that poly(rG) was not included as it may form complex secondary structures. (C) Increasing amounts (10-, 100- or 500-fold molar excess) of the unlabelled Δ1124–1224 nt transcript (lanes 1–4), Δ1075–1149 nt transcript (lanes 5–8), or Δ1150–1224 nt transcript (lanes 9–13) were added to 2 μg of recombinant AnxA2 to compete with 150 fmol of the corresponding uniformly radiolabelled transcripts. (D) The unlabelled Δ1124–1224 nt transcript was either excluded or added in 500-fold excess to 2 μg of recombinant AnxA2 to compete with 50 fmol of the uniformly radiolabelled Δ1075–1149 nt (lanes 13 and 14) and Δ1150–1224 nt (lanes 15 and 16) transcripts. 1 μg/μl yeast tRNA was present to inhibit non-specific RNA binding in all reactions. Binding was performed as described in Materials and methods.
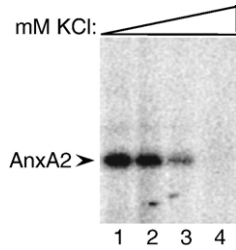
Fig. 5. The effect of increasing KCl concentration on the binding of *anx*A2 mRNA to its cognate protein. 2 fmol of radiolabelled in vitro transcribed *anx*A2 mRNA was incubated with 2 μg AnxA2t in the presence of 50 (lane 1), 100 (lane 2), 200 (lane 3) or 500 (lane 4) mM KCl. Binding was performed as described in Materials and methods.

the interaction of mRNA with AnxA2. This suggestion is corroborated by the finding that the Δ1150–1224 nt transcript (Fig. 3D, transcript 13) interacted with AnxA2 more weakly than the Δ1124–1224 nt transcript (Fig. 3D, transcript 10). However, a transcript corresponding to this short 26 nt sequence was not able to bind to AnxA2 (Fig. 3D, transcript 12).

To further examine whether *anx*A2 mRNA contains two separate AnxA2 binding sites, competition experiments were conducted in which unlabelled full-length *anx*A2 mRNA and its 3′-UTR competed with the radiolabelled full-length *anx*A2 mRNA transcript for binding to AnxA2 (Fig. 4A). Effective competition was observed at 100-fold molar excess of unlabelled *anx*A2 mRNA (Fig. 4A, lane 4). By contrast, the unlabelled 3′-UTR transcript did not significantly compete with the full-length *anx*A2 mRNA (Fig. 4A, lanes 5–8), suggesting that the mRNA contains two independent AnxA2 binding regions. Further competition experiments, using radiolabelled *anx*A2 mRNA, were performed with ssRNA or dsRNA of random size (Fig. 4B, lanes 9–13). The results suggested that ssRNA homopolymers are more efficient competitors than the poly(rI-rC) dsRNA. Poly(rG) was not tested as G-rich sequences are known to form complex secondary structures [37]. On average (mean values from 3 independent experiments), mRNA binding to AnxA2 was reduced to $41\pm2\%$, $24\pm4\%$, $36\pm4\%$ and $67\pm5\%$ of the control values when the binding of radiolabelled *anx*A2 mRNA was competed by the presence of ss poly(rA), ss poly(rU), ss poly(rC) and ds poly(rI-rC) homopolymers, respectively. These data support the conclusion that the AnxA2-binding region of the *anx*A2

mRNA has both ss and ds character, with a possible weak preference for U-rich sequences. However, complete competition was not observed with any of the homopolymers, indicating that specific higher order mRNA structures are involved in the AnxA2–mRNA complex formation. The presence of uridine in the AnxA2-binding region was also supported by the UV cross-linking experiments in which the signal observed on instant imaging, is due to the UV cross-linked [^{32}P]-labelled uridine nucleotides bound to AnxA2. Since the relative electrophoretic mobility of nucleotide-bound AnxA2 did not significantly change, it appears that only a few nucleotides could be UV cross-linked to AnxA2 (data not shown).

To obtain further information on the identity of the specific AnxA2-binding 3′-UTR region of the *anx*A2 mRNA, additional competition experiments were performed. Thus, in these experiments three different unlabelled transcripts of the 1075–1224 nt 3′-UTR region of *anx*A2 mRNA (transcripts 10, 11 and 13) were used at 10-, 100- and 500-fold molar excess, to compete with the corresponding radiolabelled transcripts (Fig. 4C). It is evident that only the Δ1124–1224 nt transcript (transcript 10) competed effectively (Fig. 4C, lanes 1–4), suggesting that most of this region is required for specific interaction with AnxA2. The finding that the unlabelled Δ1124–1224 nt transcript (transcript 10) was also able to compete for the binding of the radiolabelled Δ1075–1149 nt (transcript 11) and Δ1150–1224 nt (transcript 13) transcripts (Fig. 4D, lanes 13–14 and 15–16, respectively), further support this conclusion.

High concentrations of KCl completely abolished the binding of *anx*A2 mRNA to the AnxA2t (Fig. 5), indicating that electrostatic interactions are crucial for the interaction. These forces are most likely contributed by basic amino acids and the phosphate backbone of RNA [38]. The interaction was preserved at physiological KCl concentrations.

To compare the 3′-UTRs of *anx*A2 mRNA in different mammalian species, an alignment of the nucleotide sequences was performed (Fig. 6). In agreement with the binding data, showing that the 86 nt localisation signal of mouse c-*myc* mRNA [17] and the 1124–1224 nt region of *anx*A2 mRNA (present results) are involved in interaction with AnxA2, a five nucleotide consensus sequence, 5′-AA(C/G)(A/U)G, could be identified in these regions (Fig. 6). This sequence is repeated
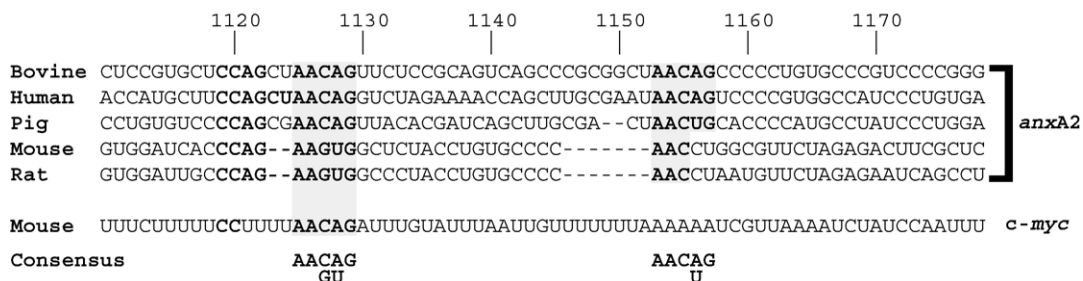

Fig. 6. Alignment of partial 3′-UTR regions of *anx*A2 mRNAs from different mammalian species and mouse c-*myc* mRNA. The two repeats of the consensus sequence are indicated in grey. The numbers above refer to the nucleotide sequence of bovine *anx*A2 mRNA.

once in the bovine, human and porcine 3′-UTRs of *anx*A2 mRNA, whereas the repeat in the mouse and rat sequences appears to be degenerated. Moreover, the 3′-UTRs of *anx*A2 mRNAs contain a common sequence, CCAG, which is not present in the localisation signal of c-*myc* mRNA (Fig. 6, in bold). It appears to be unrelated to the interaction with AnxA2 since it is located in the non-binding Δ1075–1123 nt region. However, it could represent a *cis*-acting sequence for another *trans*-acting factor.

4. Discussion

4.1. The interaction of AnxA2 with its cognate mRNAs involves the 3′-UTR

We have previously shown that AnxA2 is a mRNA-binding protein associated with CBP of Krebs II cells [15]. This finding indicated that specific AnxA2-associated mRNAs are bound to cytoskeleton elements and translated on CBPs. One of these specific mRNAs is c-*myc* [24], which binds to AnxA2 via the localisation signal in its 3′-UTR [17]. The presence of c-*myc* mRNA in AnxA2-containing mRNP complexes has been confirmed by an independent study [16].

In the present study we show that AnxA2 interacts with specific mRNAs in the CBP fraction and identify two such mRNAs as *anx*A2 and c-*myc* mRNAs (Figs. 1 and 2). Immunoprecipitation of AnxA2 from cell fractions, followed by RT-PCR of the AnxA2-associated RNAs using specific primers, revealed that these mRNAs, but not β_2-*microglobulin* mRNA, are present in the AnxA2-associated mRNP complexes (Fig. 2), indicating that this interaction is specific for a subset of cellular mRNAs. These results are in accordance with recent data showing that structurally and/or functionally related mRNAs are transported together in large mRNP complexes [39]. The localisation signal in the AnxA2-binding 3′-UTR of c-*myc* mRNA [17], forms a stem–loop structure that targets the mRNA to CBP in the perinuclear region for translation [40,41]. Also *anx*A2 mRNA is translated on CBP (Figs. 1 and 2), suggesting that it contains a similar stem–loop structure in its 3′-UTR.

To identify the sequence elements in *anx*A2 mRNA involved in its binding to AnxA2, several truncated forms of *anx*A2 mRNA were generated. Collectively, the in vitro binding studies (Figs. 3B and 4A) suggest the presence of two independent binding regions in full-length *anx*A2 mRNA. One such region resides in the 3′-UTR and another possibly in the 5′-UTR, enabling AnxA2 to interact with both regulatory ends of the mRNA. UTRs at both termini of mRNA are known to interact via associated proteins such as poly(A)-binding protein and initiation factor 4G [42,43]. Furthermore, by binding to *trans*-acting proteins, the 5′-UTR is mainly involved in modulating initiation of translation, while the 3′-UTR is primarily involved in mRNA transport and stability [44]. AnxA2 does not seem to play a role in mRNA stability since binding of AnxA2 to c-*myc* mRNA or its cognate mRNA in cell lysates has no effect on mRNA degradation in vitro (unpublished results). Translation is repressed during mRNA transport to ensure specific targeting of

proteins. Thus, it is possible that AnxA2 functions in both localisation and repression of translation during transport of specific mRNAs.

Further binding studies, using different short truncated transcripts of the 3′-UTR, indicated that the 1124–1224 nt region of *anx*A2 mRNA is involved in the binding to its cognate protein (Fig. 3C and D, compare transcripts 9–13). Competition studies corroborate this proposal since only the entire 1124–1224 nt transcript (transcript 10) was able to compete for the other AnxA2-binding transcripts (transcripts 11 and 13) of the 3′-UTR of *anx*A2 mRNA (Fig. 4D). The interaction with AnxA2 appeared to essentially involve the 1124–1149 nt region, which may form a putative stem–loop structure, although a short transcript corresponding to this region was not able to bind to AnxA2 (Fig. 3D, transcript 12), most likely due to its inability to form a particular higher order structure or due to the formation of an equilibrium of metastable RNA structures of low energy. Interestingly, this short region contains a putative binding motif of five nucleotides, 5′-AA(C/G)(A/U) G, that appears twice within this 100 nt sequence (Δ1124–1224 nt transcript) (Fig. 6) and most likely is part of a specific higher order RNA structure. The Δ1150–1224 nt transcript (transcript 13) that interacts only weakly with AnxA2 contains only the second repeat, suggesting that the first one in the Δ1124–1149 nt region represents the principal AnxA2-binding region. However, the second repeat may also contribute to the interaction since the Δ1124–1224 nt transcript (transcript 10) is able to compete for the Δ1075–1149 nt transcript (transcript 11) (Fig. 4D). Repeated binding motifs have been implicated in the targeting of other mRNAs such as *Vg1* or *VegT* [45]. In general, most perinuclear mRNA localisation signals have been delimited to 100–200 nt [28,40,46] and the signal in the 3′-UTR of *anx*A2 mRNA appears to be of the same size. Notably, the five-nucleotide consensus sequence (AACAG) is also present in the 86 nt localisation signal of mouse c-*myc* mRNA, which was previously found to interact with AnxA2 [17]. Furthermore, the perinuclear localisation signal in the 3′-UTR of *vimentin* mRNA [46] that is translated on CBP (unpublished results), contains two repeats of this consensus sequence. However, the perinuclear localisation signals of the mouse slow/cardiac *troponin* C and chicken α-cardiac *actin* mRNAs [47] lack this sequence, suggesting that it may target mRNAs to CBP, outside the perinuclear region.

Several lines of evidence support the conclusion that the interaction of AnxA2 with *anx*A2 and c-*myc* mRNAs is specific. Firstly, β_2-*microglobulin* mRNA was not associated with immunoprecipitated AnxA2 (Fig. 2A). Secondly, AnxA2 does not bind to the coding region of its cognate mRNA nor to the Δ1075–1123 nt, Δ1122–1143 nt or Δ1225–1381 nt transcripts (transcripts 9, 12 and 8, respectively) of the 3′-UTR. Thirdly, the binding is not caused by non-specific mRNA–AnxA2 interactions since BSA (Fig. 3), recombinant p11, α-actin and denatured AnxA2 did not show any binding (data not shown). Finally, a high concentration of tRNA (1 μg/μl) was present in the binding assays to prevent non-specific RNA–protein interactions and we have previously reported that AnxA2 does not bind rRNA [15].

4.2. The binding of mRNAs to AnxA2 involves higher order RNA structures

Using the Mfold programme we were not able to predict an identical RNA secondary structure either for the aligned sequences shown in Fig. 6 or the entire 3′-UTR of the same mRNAs. Also, previous prediction of secondary structures in c-*myc* mRNA from several species failed to identify identical stem–loop structures, regardless of a rather long consensus sequence [40]. However, both rat and mouse *anx*A2 mRNAs interact with AnxA2 (unpublished results), indicating that a specific secondary structure of the 3′-UTR is required for binding. In favour of this suggestion, mutating the GUAUUUA sequence in the localisation signal of c-*myc* mRNA, leading to disruption of a secondary stem–loop structure, also partially abolished its interaction with AnxA2 [17]. Moreover, the presence of 30% (v/v) formamide in the binding assay, which destroys secondary structures in mRNA, greatly diminished their binding to AnxA2, while Mg^{2+}, which promotes the formation and stabilisation of RNA secondary structures, enhanced the binding (data not shown).

Previous well-known RNA–protein interactions have been demonstrated to rely mainly upon higher order structures [48]. For example, mutations disrupting the formation of the stem–loop structure in the localisation signal in the 3′-UTR of *K10* mRNA all block its localisation to the anterior pole of the *Drosophila* oocyte. By contrast, mutations that alter only the nucleotide sequence have little or no effect on the localisation of this mRNA [49]. In the present study, competition with both ssRNA or dsRNA polymers partially inhibited the binding of both full-length *anx*A2 (Fig. 4B) and c-*myc* mRNAs (unpublished results) to AnxA2, with the ssRNA homopolymers being the most effective competitors. Thus, the binding of these mRNAs to AnxA2 appears to involve their higher order structure including both ssRNA and dsRNA regions.

Based on these results, we conclude that cells contain a distinct pool of AnxA2 that is an integral component of mRNP complexes associated with the cytoskeleton, and suggest that it functions in the transport and targeting of specific mRNAs. This proposal is further supported by the demonstration that AnxA2 also acts as a nuclear shuttle protein [50,51] and that it binds to the localisation signal of c-*myc* mRNA [17], which is translated on CBP [15]. Importantly, the present results indicate that a region of about 100 nucleotides in the 3′-UTR of *anx*A2 mRNA is involved in the interaction with its cognate protein. This region contains a specific higher order RNA structure and two repeats of a five nucleotide consensus sequence, 5′-AA(C/G)(A/U)G. The interaction of AnxA2 with its cognate mRNA may imply a post-transcriptional feed-back mechanism that ultimately regulates the synthesis of the protein.

References

[1] D. St. Johnston, Moving messages: the intracellular localization of mRNAs, Nat. Rev., Mol. Cell Biol. 6 (2005) 363–375.

[2] M.J. Moore, From birth to death: the complex lives of eukaryotic mRNAs, Science 309 (2005) 1514–1518.

[3] J. Condeelis, R.H. Singer, How and why does beta-actin mRNA target? Biol. Cell 97 (2005) 97–110.

[4] Y. Shav-Tal, R.H. Singer, RNA localization, J. Cell. Sci. 118 (2005) 4077–4081.

[5] E.H. Kislauskis, Z. Li, R.H. Singer, K.L. Taneja, Isoform-specific 3′-untranslated sequences sort alpha-cardiac and beta-cytoplasmic actin messenger RNAs to different cytoplasmic compartments, J. Cell Biol. 123 (1993) 165–172.

[6] K.L. Mowry, C.A. Cote, RNA sorting in *Xenopus* oocytes and embryos, FASEB J. 13 (1999) 435–445.

[7] L. Allen, M. Kloc, L.D. Etkin, Identification and characterization of the Xlsirt cis-acting RNA localization element, Differentiation 71 (2003) 311–321.

[8] J.H. Carson, S. Kwon, E. Barbarese, RNA trafficking in myelinating cells, Curr. Opin. Neurobiol. 8 (1998) 607–612.

[9] S.E. Bergsten, E.R. Gavis, Role for mRNA localization in translational activation but not spatial restriction of nanos RNA, Development 126 (1999) 659–669.

[10] A.F. Ross, Y. Oleynikov, E.H. Kislauskis, K.L. Taneja, R.H. Singer, Characterization of a β-*actin* mRNA zipcode-binding protein, Mol. Cell. Biol. 17 (1997) 2158–2165.

[11] Z. Elisha, L. Havin, I. Ringel, J.K. Yisraeli, Vg1 RNA binding protein mediates the association of Vg1 RNA with microtubules in *Xenopus* oocytes, EMBO J. 14 (1995) 5109–5114.

[12] V. Gerke, K. Weber, Identity of p36K phosphorylated upon *Rous sarcoma* virus transformation with a protein purified from brush borders: calcium-dependent binding to non-erythroid spectrin and F-actin, EMBO J. 3 (1984) 227–233.

[13] N.W. Ikebuchi, D.M. Waisman, Calcium-dependent regulation of actin filament bundling by lipocortin-85, J. Biol. Chem. 265 (1990) 3392–3400.

[14] M.J. Hayes, D. Shao, M. Bailly, S.E. Moss, Regulation of actin dynamics by annexin 2, EMBO J. 25 (2006) 1816–1826.

[15] A. Vedeler, H. Hollås, Annexin II is associated with mRNAs which may constitute a distinct subpopulation, Biochem. J. 348 (2000) 565–572.

[16] N.R. Filipenko, T.J. MacLeod, C.S. Yoon, D.M. Waisman, Annexin A2 is a novel RNA-binding protein, J. Biol. Chem. 279 (2004) 8723–8731.

[17] I. Mickleburgh, B. Burtle, H. Hollås, G. Campbell, Z. Chrzanowska-Lightowlers, A. Vedeler, J. Hesketh, Annexin A2 binds to the localization signal in the 3′ untranslated region of c-myc mRNA, FEBS J. 272 (2005) 413–421.

[18] V. Gerke, S.E. Moss, Annexins: from structure to function, Physiol. Rev. 82 (2002) 331–371.

[19] U. Rescher, V. Gerke, Annexins—Unique membrane binding proteins with diverse functions, J. Cell. Sci. 117 (2004) 2631–2639.

[20] S.E. Moss, R.O. Morgan, The annexins, Genome Biol. 5 (2004) 219.1–219.8.

[21] M.J. Hayes, U. Rescher, V. Gerke, S.E. Moss, Annexin–actin interactions, Traffic 5 (2004) 571–576.

[22] V. Gerke, C.E. Creutz, S.E. Moss, Annexins: linking Ca^{2+} signalling to membrane dynamics, Nature Rev. 6 (2005) 449–461.

[23] A. Vedeler, I.F. Pryme, J.E. Hesketh, The characterization of free, cytoskeletal-bound and membrane-bound polysomes in Krebs II ascites and 3T3 cells, Mol. Cell. Biochem. 100 (1991) 183–193.

[24] A. Vedeler, I.F. Pryme, J.E. Hesketh, The compartmentalization of polysomes into free, cytoskeletal-bound and membrane-bound populations, Biochem. Soc. Trans. 19 (1991) 1108–1111.

[25] J.E. Hesketh, G.P. Campbell, P.F. Whitelaw, c-*myc* mRNA in cytoskeletal-bound polysomes in fibroblasts, Biochem. J. 274 (1991) 607–609.

[26] R. Moss, I.F. Pryme, A. Vedeler, Free, cytoskeletal-bound and membrane-bound polysomes isolated from MPC-11 cells and Krebs II ascites cells differ in their complement of poly(A) binding proteins, Mol. Cell. Biochem. 131 (1994) 131–139.

[27] G. Montana, A. Bonura, D.P. Romancino, E. Sbisa, M.A. Di Carlo, A 54-kDa protein specifically associates the 3′ untranslated region of three maternal mRNAs with the cytoskeleton of the animal part of the *Paracertrotus lividus* egg, Eur. J. Biochem. 247 (1997) 183–189.

[28] G. Dalgleish, J.L. Veyrune, J.M. Blanchard, J.E. Hesketh, mRNA localization by a 145-nucleotide region of the c-*fos* 3′-untranslated region—Links to translation but not stability, J. Biol. Chem. 276 (2001) 13593–13599.

[29] A.O. Gramolini, G. Belanger, B.J. Jasmin, Distinct regions in the 3′ untranslated region are responsible for targeting and stabilizing utrophin transcripts in skeletal muscle cells, J. Cell Biol. 154 (2001) 1173–1183.

[30] P. Chomczynski, N. Sacchi, Single-step method of RNA isolation by acid guanidinium thiocyanate–phenol–chloroform extraction, Anal. Biochem. 162 (1987) 156–159.

[31] E. Chu, T. Cogliati, S.M. Copur, A. Borre, D.M. Voeller, C.J. Allegra, S. Segal, Identification of in vivo target RNA sequences bound by thymidylate synthase, Nucleic Acids Res. 24 (1996) 3222–3228.

[32] T. Kristensen, C.J.M. Saris, T. Hunter, L.J. Hicks, D.J. Noonan, J.R. Glenney, B.F. Tack, Primary structure of bovine calpactin I heavy chain (p36), a major cellular substrate for retroviral protein-tyrosine kinases: homology with the human phospholipase A_2 inhibitor lipocortin, Biochem. 25 (1986) 4497–4503.

[33] U.K. Laemmli, Cleavage of structural proteins during assembly of the head of bacteriophage T4, Nature 227 (1970) 680–685.

[34] Y.K. Kwon, N.B. Hecht, Cytoplasmic protein binding to highly conserved sequences in the 3′ untranslated region of mouse protamine 2 mRNA, a translationally regulated transcript of male germ cells, Proc. Natl. Acad. Sci. U. S. A. 88 (1991) 3584–3588.

[35] D.H. Mathews, J. Sabina, M. Zuker, D.H. Turner, Expanded sequence dependence of thermodynamic parameters improves prediction of RNA secondary structure, J. Mol. Biol. 288 (1999) 911–940.

[36] M. Zuker, Mfold web server for nucleic acid folding and hybridization prediction, Nucleic Acids Res. 31 (2003) 3406–3415.

[37] V. Dapic, V. Abdomerovic, R. Marrington, J. Peberdy, A. Rodger, J.O. Trent, P.J. Bates, Biophysical and biological properties of quadruplex oligodeoxyribonucleotides, Nucleic Acids Res. 31 (2003) 2097–2107.

[38] M.J. Law, M.E. Linde, E.J. Chambers, C. Oubridge, P.S. Katsamba, L. Nilsson, I.S. Haworth, I.A. Laird-Offringa, The role of positively charged amino acids and electrostatic interactions in the complex of U1A protein and U1 hairpin II RNA, Nucleic Acids Res. 34 (2006) 275–285.

[39] J.D. Keene, P.J. Lager, Post-transcriptional operons and regulons co-ordinating gene expression, Chromosome Res. 13 (2005) 327–337.

[40] J.L. Veyrune, G.P. Campbell, J. Wiseman, J.M. Blanchard, J.E. Hesketh, A localisation signal in the 3′ untranslated region of c-myc mRNA targets c-myc mRNA and beta-globin reporter sequences to the perinuclear cytoplasm and cytoskeletal-bound polysomes, J. Cell. Sci. 109 (1996) 1185–1194.

[41] H. Chabanon, I. Mickleburgh, B. Burtle, C. Pedder, J. Hesketh, An AU-rich stem–loop structure is a critical feature of the perinuclear localization signal of c-*myc* mRNA, Biochem. J. 392 (2005) 475–483.

[42] A. Kahvejian, G. Roy, N. Sonenberg, The mRNA closed-loop model: the function of PABP and PABP-interacting proteins in mRNA translation, Cold Spring Harbor Symp. Quant. Biol. 66 (2001) 293–300.

[43] B. Mazumder, V. Seshadri, P.L. Fox, Translational control by the 3′-UTR: the ends specify the means, Trends Biochem. Sci. 28 (2005) 91–98.

[44] G.S. Wilkie, K.S. Dickson, N.K. Gray, Regulation of mRNA translation by 5′- and 3′-UTR-binding factors, Trends Biochem. Sci. 28 (2003) 182–188.

[45] M. Bubunenko, T.L. Kress, U.D. Vempati, K.L. Mowry, M.L. King, A consensus RNA signal that directs germ layer determinants to the vegetal cortex of *Xenopus* oocytes, Dev. Biol. 248 (2002) 82–92.

[46] G. Bermano, R.K. Shepherd, Z.E. Zehner, J.E. Hesketh, Perinuclear mRNA localisation by vimentin 3′-untranslated region requires a 100 nucleotide sequence and intermediate filaments, FEBS Lett. 497 (2001) 77–81.

[47] K.K. Reddy, F.M. Oitomen, G.P. Patel, J. Bag, Perinuclear localization of slow troponin C mRNA in muscle cells is controlled by a *cis*-element located at its 3′ untranslated region, RNA 11 (2005) 294–307.

[48] F. Mignone, C. Gissi, S. Liuni, G. Pesole, Untranslated regions of mRNAs, Genome Biol. 3 (2002) 0004.1–0004.10.

[49] T.L. Serano, R.S. Cohen, A small predicted stem–loop structure mediates oocyte localization of *Drosophila K10* mRNA, Development 121 (1995) 3809–3818.

[50] D.A. Eberhard, L.R. Karns, S.R. VandenBerg, C.E. Creutz, Control of the nuclear-cytoplasmic partitioning of annexin II by a nuclear export signal and by p11 binding, J. Cell. Sci. 114 (2001) 3155–3166.

[51] J. Liu, C.A. Rothermund, J. Ayala-Sanmartin, J.K. Vishwanatha, Nuclear annexin II negatively regulates growth of LNCaP cells and substitution of ser 11 and 25 to glu prevents nucleo-cytoplasmic shuttling of annexin II, BMC Biochem. 4 (2003) 10.